

18 a 21 de novembro de 2014, Caldas Novas - Goiás

## ACOUSTIC PROPAGATION EVALUATION USING TRADITIONAL FINITE DIFFERENCES AND DISPERSION RELATION PRESERVING (DRP)

Paulo Alfredo Mainieri Junior, paulojrudi@yahoo.com.br  
Odenir de Oliveira, odenir@mecanica.ufu.br<sup>2</sup>  
Aristeu da Silveira Neto, aristeus@mecanica.ufu.br<sup>3</sup>

<sup>1</sup>Federal University of Uberlandia – Mechanical Engineering Faculty – Fluid Mechanics Laboratory  
Av. Joao Naves de Avila 2121 – Campus Santa Monica – Uberlandia – MG – 38408-100

<sup>2</sup>Federal University of Uberlandia – Mechanical Engineering Faculty – Fluid Mechanics Laboratory  
Av. Joao Naves de Avila 2121 – Campus Santa Monica – Uberlandia – MG – 38408-100

<sup>3</sup>Federal University of Uberlandia – Mechanical Engineering Faculty – Fluid Mechanics Laboratory  
Av. Joao Naves de Avila 2121 – Campus Santa Monica – Uberlandia – MG – 38408-100

**Abstract:** *The main purpose of this work is the evaluation of spatial schemes used on CAA (Computational AeroAcoustic): Traditional finite differences, and DRP (Dispersion Relation Preserving), on 1D (one dimension) acoustic propagation prediction. A secondary goal is to present details of construction of DRP, proposed by Tam and Webb (1993) and advantages of this schemes over traditional finite differences schemes. Temporal schemes as Euler, Runge-Kutta 2<sup>nd</sup> and 4<sup>th</sup> order methods and CAA optimized methods such as LDDRK and RK46-NL will be evaluated. This work shows an outstanding efficiency of Runge-Kutta 2<sup>nd</sup> order over Runge-Kutta 4<sup>th</sup> order scheme, and in some cases, even superior to the optimized CAA schemes. The simulations revealed that DRP loss efficiency over traditional finite differences scheme when grid refinement occurs.*

**Keywords:** *DRP, acoustic propagation, finite differences, Runge-Kutta.*

### 1. INTRODUCTION

The stream noise generated by the air over trees, rocks and other obstacles always interested researchers along the centuries. Older studies of the phenomenon goes back to the ancient Greece and the term eolian is used to describe that behavior. In modern age, names as Vincent Strouhal left a great legacy on the development of this science, studying the sound generated by air streams through wires (aeolian tones).

A few decades later, the aeroacoustic emerges as a branch of fluid mechanics interested in sound generation and its propagation of air flowing over flat surfaces. Once more, a practical problem guides the research efforts to this area. In this case the primary motivation was the start operation of the noise turbojets after second world war, in the decades of 1950 and 1960, mostly in north america and europe continents.

In fact, the fast growing of the aviation using reaction engines (also called turbojets), the problem of the noise generated by high speed exhaust gas flow became an inconvenience for the society, a hard psychological and physiological impact in the people living close by large airports, for example, Heatrow, in London, and JFK, in New York.

The intense engine noise is created by the interface of exhaust gas flow and the atmospheric air, due a strong shear strength of the velocity gradient between the two flows, like the sound produced when two smooth surfaces are rubbed one against the other.

In this scenario of crisis born the aeroacoustic, with the first works of Sir James Lighthill. Lighthill deduced a transport equation from Navier-Stokes equations describing the specific mass fluctuation in an outflow. Under certain conditions the analytical solution of this equation enable to determine the sound propagation to a far field, away from the sound source. Moreover, following his researches, Lighthill also demonstrate that the intense of the aerodynamic

noise is proportional to the relative velocity between the exhaust gas flow and the atmospheric air, elevated to the power of 8.

As a result of these first studies the aeronautic industry created the turbofan engines, that were nothing more than the turbojet engines now equipped with a huge inlet air to supply the engine, and also to cover the exhaust gas flow with a coat, faster than static (or quasi static) atmospheric air and slower than the exhaust gas, decreasing the shear stress between those flows.

Surpassed the first obstacles, the daily coexistence shows other noise sources apart of the engines. The airflow passing through the aircraft's body, the high lift devices, the landing gear and the wing tips, proved to be sources of noise so intense as the turbofan engines.

In-depth studies revealed that the turbojets generated noises in order of 115 dB (decibel). The air pressure gradient due sound propagation, even close to the engine, was very small, about  $10^{-4}$  of the atmospheric pressure. Although the sound generation and its propagation depend on the same variables, the order of magnitude of those variables for the same phenomena are too disparate. To solve the sound generation together with its propagation requires a refined control error, a very high computational cost even in these days, and for that time, unthinkable. To solve the sound generation means to solve the flow (aerodynamics), to solve the turbulence present in the flow. From the point of view of the fluid mechanics, the best way to do this is by DNS (Direct Numerical Simulation), solving Navier-Stokes equations completely. But, even through the powerful moderns computers, this task is only possible for very simple cases, for very low Reynolds numbers. To solve the turbulence without solve all its scales (RANS, URANS, LES...), is still under discussion because of the required filtration, which eliminates a very large band of sound frequencies. To solve the turbulence in all scales requires a very refined mesh, even in a little domain, is still impractical for most of engineering problems. To add to the solution the sound propagation, in a far field (extremely large mesh), elevates the computational efforts beyond the current technological capability.

Lighthill's research brought a perception that was possible to separate sound propagation from its generation if the flow had a very low Mach number. His studies revealed also the low influence of air viscosity for propagation purposes, far from source sound generation (low Mach number). This fact reduced the costs of the heavy computational processing, turning the Navier-Stokes equations into Euler equations.

Many sound propagation schemes have been proposed over the years to solve the first order spatial partial derivative of the sound equation. Minimize the error under a low computational cost is the main objective of all schemes, but some of them has add a very simple implementation to its profile. In computational aeroacoustic (CAA) the finite differences technique has been detached.

Based on Taylor series this simple technique has reached good efficiency. The focus of these techniques is to minimize the sound dissipation error (energy loss) but, for the fact that it is an approximation of the real value of the variable, the imprecision of the scheme stimulates the growing of an artificial sound dispersion. So it has been created by Tam and Webb (1993) a finite differences schemes to inhibit this dispersion growing, among them stands out the DRP (Dispersion Relation Preserving).

On the basis of the above, this work has the main objective to evaluate the performance of these two groups of spatial schemes (finite differences and DRP) together with temporal schemes (Euler method, 2nd and 4th order Runge-Kutta and the CAA optimized methods: LDDRK and RK46-NL) on 1D (one dimension) acoustic pulse propagation, comparing results with analytical data and show a brief deduction of DRP schemes.

## 2. GOVERNING EQUATIONS

### 2.1. Acoustic Propagation Equations

As shown by Mainieri et al. (2013), the set of equations of the acoustic propagation for a quasi-static flow with Reynolds number  $< 1000$  are presented by eq. (2) for 1D (one dimension) case:

$$1D: \begin{cases} \frac{\partial u}{\partial t} + M_x \frac{\partial u}{\partial x} + \frac{\partial p}{\partial x} = 0 \\ \frac{\partial p}{\partial t} + M_x \frac{\partial p}{\partial x} + \frac{\partial u}{\partial x} = 0 \end{cases} \quad (1)$$

where  $u$  is the velocity in  $x$  direction,  $p$  is the pressure,  $t$  is the time and  $M_x$  is the velocity propagation of the acoustic pulse in relation to the sound speed.

That set of equations were nondimensionalized as described by Mainieri et al. (2013).

### 2.2. Spatial Derivatives

The spatial derivatives were solved by finite differences or by DRP. The deduction of both schemes is explained in detail in Mainieri et al. (2013). The coefficients of the finite differences schemes are shown in Tab. 1 and for DRP schemes in Tab. 2. In this work it was adopted central schemes due its looseness property.

**Table 1. Coefficients for central finite differences schemes.**

Points/Order	2 <sup>a</sup>	4 <sup>a</sup>	6 <sup>a</sup>	8 <sup>a</sup>	10 <sup>a</sup>	12 <sup>a</sup>
$a_{-6}$						1/5544
$a_{-5}$					-1/1260	-1/385
$a_{-4}$				1/280	5/504	1/56
$a_{-3}$			-1/60	-4/105	-5/84	-5/63
$a_{-2}$		1/12	3/20	1/5	5/21	15/56
$a_{-1}$	-1/2	-2/3	-3/4	-4/5	-5/6	-6/7
$a_0$	0	0	0	0	0	0
$a_{+1}$	1/2	2/3	3/4	4/5	5/6	6/7
$a_{+2}$		-1/12	-3/20	-1/5	-5/21	-15/56
$a_{+3}$			1/60	4/105	5/84	5/63
$a_{+4}$				-1/280	-5/504	-1/56
$a_{+5}$					1/1260	1/385
$a_{+6}$						-1/5544

**Table 2. Coefficients for central DRP schemes.**

Points/Order	2 <sup>a</sup>	4 <sup>a</sup>	6 <sup>a</sup>
$a_{-4}$			0.005939804
$a_{-3}$		-0.0265199521	-0.052305492
$a_{-2}$	0.123171607	0.189413142	0.233157260
$a_{-1}$	-0.746343213	-0.799266427	-0.833157260
$a_0$	0	0	0
$a_{+1}$	0.746343213	0.799266427	0.833157260
$a_{+2}$	-0.123171607	-0.189413142	-0.233157260
$a_{+3}$		0.0265199521	0.052305492
$a_{+4}$			-0.005939804

### 2.3. Temporal Derivatives

The temporal derivatives were solved by:

- Euler's method (1<sup>a</sup> order) (EULER),
- Runge-Kutta 2<sup>nd</sup> order (RK2),
- Runge-Kutta 4<sup>th</sup> order (RK4),
- LDDRK (optimized method of 2<sup>nd</sup> order for nonlinear problems and 4<sup>th</sup> order for linear problems),
- RK46-NL (optimized method of 4<sup>th</sup> order for linear and nonlinear problems).

The Euler and Runge-Kutta methods requires no detailed comments because of its widespread use and well known by specialized literature. LDDRK (Low Dispersion low Dissipation Runge-Kutta) is a Runge-Kutta optimized method for aeroacoustic developed by Hu et al. (1996). RK46-NL is also a Runge-Kutta optimized method for aeroacoustic (46-NL – 4<sup>th</sup> order and 6 steps NonLinear problems) developed by Berland et al. (2006).

### 2.4. Absolute Error

As the main purpose of this work is to present in a clear and unambiguous manner concepts and ideas of acoustic propagation, it was chosen the simpler kind of error, the absolute error, defined as:

$$Error = |Analytical Value - Numeric Value| \tag{2}$$

It is important to remember that there is no damping function inside the computer code in order to not minimize numeric fluctuations.

### 3. CONSTRUCTING DRP

Taking the general formula for finite differences schemes:

$$\frac{\partial f(x)}{\partial x} \cong \frac{1}{\Delta x} \sum_{j=N}^M (a_j \cdot f(x + j \cdot \Delta x)) \quad (3)$$

and transporting it to Fourier spectral space:

$$i \cdot k \cdot \hat{f}_k \cong \left[ \frac{1}{\Delta x} \sum_{j=N}^M (a_j \cdot e^{ikj\Delta x}) \right] \hat{f}_k \quad (4)$$

Remembering that even in spectral space the expression of Eq. (4) still remain an approximation of the variable. The left side has the wave number  $k$ , which describes the real wavelength of the exact spatial derivative. The sum of the right side of Eq. (5) can be describe as:

$$i \cdot k^* \cdot \hat{f}_k = \left[ \frac{1}{\Delta x} \sum_{j=N}^M (a_j \cdot e^{ikj\Delta x}) \right] \hat{f}_k \quad (5)$$

Note that the wave number is no longer  $k$  but  $k^*$ , and that the expression is now an equality instead of an approximation.  $k^*$  is known as efective wave number, an approximation of the real wave number  $k$ , which is a wave number produced by the finite differences scheme.  $k^*$ is now defined as:

$$k^* = \frac{-i}{\Delta x} \sum_{j=N}^M (a_j \cdot e^{ikj\Delta x}) \quad (6)$$

The purpose of DRP scheme is to make  $k^*$ as close as possible of  $k$ . The dispersion relation is a function of the wave number, it means that taking the effective wave number  $k^*$  equal or close as possible of the real wave number  $k$ , it will be preserving the dispersion relation of the phenomenon, which is exactly the purpose and the name of this scheme, DRP – Dispersion Relation Preserving. To get there it seeks to minimize the integral of the error:

$$E = \int_{\pi/16}^{\pi/2} |k \cdot \Delta x - k^* \cdot \Delta x|^2 d(k \cdot \Delta x) \quad (7)$$

turning the error as low as possible by minimizing the error of each coefficient  $a_j$  of Eq. (8):

$$\frac{\partial E}{\partial a_j} = 0 \quad (8)$$

The original DRP original was constructed under 7 points: Three points behind and three points forward of the interest point. For a traditional finite difference scheme using seven points it would reaches sixth order of convergence, however the DRP truncates the convergence into fourth order, as shown below (Eq. 9):

$$\begin{cases} f_{i-3} = f_i + \frac{(-3\Delta x)^1}{1!} f_i^I + \frac{(-3\Delta x)^2}{2!} f_i^{II} + \frac{(-3\Delta x)^3}{3!} f_i^{III} + \frac{(-3\Delta x)^4}{4!} f_i^{IV} + R_4(x) \\ f_{i-2} = f_i + \frac{(-2\Delta x)^1}{1!} f_i^I + \frac{(-2\Delta x)^2}{2!} f_i^{II} + \frac{(-2\Delta x)^3}{3!} f_i^{III} + \frac{(-2\Delta x)^4}{4!} f_i^{IV} + R_4(x) \\ f_{i-1} = f_i + \frac{(-\Delta x)^1}{1!} f_i^I + \frac{(-\Delta x)^2}{2!} f_i^{II} + \frac{(-\Delta x)^3}{3!} f_i^{III} + \frac{(-\Delta x)^4}{4!} f_i^{IV} + R_4(x) \\ f_{i+1} = f_i + \frac{(\Delta x)^1}{1!} f_i^I + \frac{(\Delta x)^2}{2!} f_i^{II} + \frac{(\Delta x)^3}{3!} f_i^{III} + \frac{(\Delta x)^4}{4!} f_i^{IV} + R_4(x) \\ f_{i+2} = f_i + \frac{(2\Delta x)^1}{1!} f_i^I + \frac{(2\Delta x)^2}{2!} f_i^{II} + \frac{(2\Delta x)^3}{3!} f_i^{III} + \frac{(2\Delta x)^4}{4!} f_i^{IV} + R_4(x) \\ f_{i+3} = f_i + \frac{(3\Delta x)^1}{1!} f_i^I + \frac{(3\Delta x)^2}{2!} f_i^{II} + \frac{(3\Delta x)^3}{3!} f_i^{III} + \frac{(3\Delta x)^4}{4!} f_i^{IV} + R_4(x) \end{cases} \quad (9)$$

By this all coefficients remains without an exact solution, depending of one coefficient that will be optimized by the integral of Eq. (7) and the derivative of Eq. (8).

Multiplying the first row of Eq. (9) by  $a_{-3}$ , the second by  $a_{-2}$ , the third by  $a_{-1}$ , the fourth by  $a_{+1}$ , the fifth by  $a_{+2}$  and the sixth by  $a_{+3}$ . Adding all these rows and setting the result to be 1 (one) for the sum of coefficients of the first derivative ( $f_i'$ ), and 0 (zero) for the others derivatives:

$$\begin{cases} f_i: a_{-3} + a_{-2} + a_{-1} + a_{+1} + a_{+2} + a_{+3} = 0 \\ f_i': a_{-3} \cdot \frac{(-3\Delta x)^1}{1!} + a_{-2} \cdot \frac{(-2\Delta x)^1}{1!} + a_{-1} \cdot \frac{(-\Delta x)^1}{1!} + a_{+1} \cdot \frac{(\Delta x)^1}{1!} + a_{+2} \cdot \frac{(2\Delta x)^1}{1!} + a_{+3} \cdot \frac{(3\Delta x)^1}{1!} = 1 \\ f_i'': a_{-3} \cdot \frac{(-3\Delta x)^2}{2!} + a_{-2} \cdot \frac{(-2\Delta x)^2}{2!} + a_{-1} \cdot \frac{(-\Delta x)^2}{2!} + a_{+1} \cdot \frac{(\Delta x)^2}{2!} + a_{+2} \cdot \frac{(2\Delta x)^2}{2!} + a_{+3} \cdot \frac{(3\Delta x)^2}{2!} = 0 \\ f_i''': a_{-3} \cdot \frac{(-3\Delta x)^3}{3!} + a_{-2} \cdot \frac{(-2\Delta x)^3}{3!} + a_{-1} \cdot \frac{(-\Delta x)^3}{3!} + a_{+1} \cdot \frac{(\Delta x)^3}{3!} + a_{+2} \cdot \frac{(2\Delta x)^3}{3!} + a_{+3} \cdot \frac{(3\Delta x)^3}{3!} = 0 \\ f_i^{IV}: a_{-3} \cdot \frac{(-3\Delta x)^4}{4!} + a_{-2} \cdot \frac{(-2\Delta x)^4}{4!} + a_{-1} \cdot \frac{(-\Delta x)^4}{4!} + a_{+1} \cdot \frac{(\Delta x)^4}{4!} + a_{+2} \cdot \frac{(2\Delta x)^4}{4!} + a_{+3} \cdot \frac{(3\Delta x)^4}{4!} = 0 \end{cases} \quad (10)$$

Solving the first row, the coefficient  $a_{-3}$  remains as function of  $a_{-2}$ ,  $a_{-1}$ ,  $a_{+1}$ ,  $a_{+2}$ , and  $a_{+3}$ :

$$a_{-3} = -a_{-2} - a_{-1} - a_{+1} - a_{+2} - a_{+3} \quad (11)$$

Replacing  $a_{-3}$  on second row,  $a_{-2}$  remains as function of  $a_{-1}$ ,  $a_{+1}$ ,  $a_{+2}$ ,  $a_{+3}$ :

$$a_{-2} = 1 - 2a_{-1} - 4a_{+1} - 5a_{+2} - 6a_{+3} \quad (12)$$

Doing the same process on third row,  $a_{-1}$  remains as function of  $a_{+1}$ ,  $a_{+2}$ ,  $a_{+3}$ :

$$a_{-1} = \frac{1}{2}(5 - 12a_{+1} - 20a_{+2} - 30a_{+3}) \quad (13)$$

Solving fourth row,  $a_{+1}$  remains as function of  $a_{+2}$ ,  $a_{+3}$ :

$$a_{+1} = \frac{1}{24}(11 - 60a_{+2} - 120a_{+3}) \quad (14)$$

In fifth row,  $a_{+2}$  f remains as function of  $a_{+3}$ :

$$a_{+2} = \frac{1}{12}(-1 - 48a_{+3}) \quad (15)$$

Equation (6) reveals that the effective wave number  $k^*$  is a sum of complex numbers. These complex number can be written in trigonometric form:

$$e^{i.j.k.\Delta x} = \cos(j.k.\Delta x) + i \text{sen}(j.k.\Delta x) \quad (16)$$

The integral of Eq. (7) can be written as:

$$E = \int_{\pi/16}^{\pi/2} \left| k.\Delta x - \frac{(-i)}{\Delta x} \left[ \sum_{j=-3}^3 a_j (\cos(j.k.\Delta x) + i.\text{sen}(j.k.\Delta x) +) \right] .\Delta x \right|^2 d(k.\Delta x) \quad (17)$$

Making some simplifications it becomes:

$$E = \int_{\pi/16}^{\pi/2} \left| k.\Delta x - \sum_{j=-3}^3 a_j (\text{sen}(j.k.\Delta x) - i.\cos(j.k.\Delta x)) \right|^2 d(k.\Delta x) \quad (18)$$

Open the term of sum:

$$\int_{\pi/16}^{\pi/2} \left| k.\Delta x - \left[ \begin{aligned} &a_{-3}(\sin(-3.k.\Delta x) - i.\cos(-3.k.\Delta x)) + a_{-2}(\sin(-2.k.\Delta x) - i.\cos(-2.k.\Delta x)) + \\ &a_{-1}(\sin(-1.k.\Delta x) - i.\cos(-1.k.\Delta x)) + a_{+1}(\sin(+1.k.\Delta x) - i.\cos(+1.k.\Delta x)) + \\ &a_{+2}(\sin(+2.k.\Delta x) - i.\cos(+2.k.\Delta x)) + a_{+3}(\sin(+3.k.\Delta x) - i.\cos(+3.k.\Delta x)) \end{aligned} \right] \right|^2 d(k.\Delta x) \quad (19)$$

As  $a_0$  coefficient doesn't appear in the deduction of the finite difference scheme, it means that  $a_0 = 0$ . So, the result of the integral becomes:

$$E = \frac{1}{36} \left( -\frac{320}{3} + \frac{1}{8\sqrt{2}} + \frac{1533\pi^3}{1024} + \pi \left( \frac{551}{32} - 6\cos\left[\frac{\pi}{16}\right] + \frac{3}{8}\cos\left[\frac{\pi}{8}\right] \right) + 104\sin\left[\frac{\pi}{16}\right] + 13\sin\left[\frac{\pi}{8}\right] + \frac{3}{5}a_{+3}^2(-7168 + 390\sqrt{2} + 2205\pi + 20\cos\left[\frac{\pi}{8}\right] - 192\cos\left[\frac{3\pi}{16}\right] + 5760\sin\left[\frac{\pi}{16}\right] + 900\sin\left[\frac{\pi}{8}\right] - 1600\sin\left[\frac{3\pi}{16}\right]) + \frac{3}{5}a_{+3}(-2176 + 30\sqrt{2} - 4\cos\left[\frac{3\pi}{16}\right] - 5\pi(-125 + 15\cos\left[\frac{\pi}{16}\right] - 6\cos\left[\frac{\pi}{8}\right] + \cos\left[\frac{3\pi}{16}\right]) + 1960\sin\left[\frac{\pi}{16}\right] + 80\sin\left[\frac{\pi}{8}\right] - 220\sin\left[\frac{3\pi}{16}\right]) - \frac{8}{3}\sin\left[\frac{3\pi}{16}\right] \right) \quad (20)$$

a second degree function of  $a_{+3}$  whose concavity is like a dish (minimum point).

It is interesting to note that the expression above doesn't contain any complex number. In a centered finite difference scheme the equidistant terms has the same value with opposite signals (Eq. 21):

$$a_{-n} = -a_{+n} \quad (21)$$

This behavior allow to cancel the complex numbers of equidistant terms. This information can be useful to reduce computational work on Eq. (19). Differentiating Equation (20) and setting it equal to zero it obtains  $a_{+3}$ :

$$a_{+3} = \frac{(2176 - 30\sqrt{2} - 625\pi + 75\pi\cos\left[\frac{\pi}{16}\right] - 30\pi\cos\left[\frac{\pi}{8}\right] + 4\cos\left[\frac{3\pi}{16}\right] + 5\pi\cos\left[\frac{3\pi}{16}\right] - 1960\sin\left[\frac{\pi}{16}\right] - 80\sin\left[\frac{\pi}{8}\right] + 220\sin\left[\frac{3\pi}{16}\right])}{(2(-7168 + 390\sqrt{2} + 2205\pi + 20\cos\left[\frac{\pi}{8}\right] - 192\cos\left[\frac{3\pi}{16}\right] + 5760\sin\left[\frac{\pi}{16}\right] + 900\sin\left[\frac{\pi}{8}\right] - 1600\sin\left[\frac{3\pi}{16}\right]))} = 0.0265199521 \quad (22)$$

With the value of  $a_{+3}$  it obtains  $a_{+2}$ . With  $a_{+3}$  and  $a_{+2}$  it obtains  $a_{+1}$ , and so on. Table 2, in previous section, shows some DRP coefficients.

DRP was idealized as a centered scheme. To construct a sided scheme with the same integration limits (from  $k \cdot \Delta x = \pi/16$  to  $k \cdot \Delta x = \pi/2$ ) results in the appearance of complex numbers on the error integral, not leading application of the scheme on the border of the domain or on obstacles immersed in the flow. However, using symmetric integration limits the complex coefficients are cancelled.

For a sided scheme 4-2 (four points behind and two points forward) the interior of the error integral (Eq. (19)) becomes:

$$\left| k \cdot \Delta x - \begin{bmatrix} a_{-4}(\sin(-4.k \cdot \Delta x) - i \cdot \cos(-4.k \cdot \Delta x)) + a_{-3}(\sin(-3.k \cdot \Delta x) - i \cdot \cos(-3.k \cdot \Delta x)) + \\ a_{-2}(\sin(-2.k \cdot \Delta x) - i \cdot \cos(-2.k \cdot \Delta x)) + a_{-1}(\sin(-1.k \cdot \Delta x) - i \cdot \cos(-1.k \cdot \Delta x)) + \\ a_0(\sin(0.k \cdot \Delta x) - i \cdot \cos(0.k \cdot \Delta x)) + a_{+1}(\sin(+1.k \cdot \Delta x) - i \cdot \cos(+1.k \cdot \Delta x)) + \\ a_{+2}(\sin(+2.k \cdot \Delta x) - i \cdot \cos(+2.k \cdot \Delta x)) \end{bmatrix} \right|^2 \quad (23)$$

For an integration limit  $k \cdot \Delta x = -1$ , Eq. (23) can be written as:

$$\left| -1 - \begin{bmatrix} a_{-4}(\sin(+4) - i \cdot \cos(+4)) + a_{-3}(\sin(+3) - i \cdot \cos(+3)) + \\ a_{-2}(\sin(+2) - i \cdot \cos(+2)) + a_{-1}(\sin(+1) - i \cdot \cos(+1)) + \\ a_0(\sin(0) - i \cdot \cos(0)) + a_{+1}(\sin(-1) - i \cdot \cos(-1)) + \\ a_{+2}(\sin(-2) - i \cdot \cos(-2)) \end{bmatrix} \right|^2 \quad (24)$$

Remember that now the scheme is not centered, than  $a_0 \neq 0$ . Taking the symmetric integration limit,  $k \cdot \Delta x = +1$ , the Eq. (24) is written as:

$$\left| +1 - \begin{bmatrix} a_{-4}(\sin(-4) - i \cdot \cos(-4)) + a_{-3}(\sin(-3) - i \cdot \cos(-3)) + \\ a_{-2}(\sin(-2) - i \cdot \cos(-2)) + a_{-1}(\sin(-1) - i \cdot \cos(-1)) + \\ a_0(\sin(0) - i \cdot \cos(0)) + a_{+1}(\sin(+1) - i \cdot \cos(+1)) + \\ a_{+2}(\sin(+2) - i \cdot \cos(+2)) \end{bmatrix} \right|^2 \quad (25)$$

Elevating to the square the complete expression it will appear a huge expression of complex numbers that will cancel itself for those integration limits  $[-k \cdot \Delta x, +k \cdot \Delta x]$ .

To illustrate these ideas, suppose that the expression to be square elevated is:

$$[\text{sen}(k \cdot \Delta x) - i \cos(k \cdot \Delta x)]^2 \quad (26)$$

For symmetric positions under the integration interval,

$$\begin{cases} k \cdot \Delta x = -1: [\text{sen}(-1) - i \cos(-1)]^2 \\ k \cdot \Delta x = +1: [\text{sen}(+1) - i \cos(+1)]^2 \end{cases} \quad (27)$$

it becomes:

$$\begin{cases} k \cdot \Delta x = -1: [-\text{sen}(+1) - i \cos(+1)]^2 \\ k \cdot \Delta x = +1: [+ \text{sen}(+1) - i \cos(+1)]^2 \end{cases} \quad (28)$$

Elevating to the square:

$$\begin{cases} k \cdot \Delta x = -1: [-\cos^2(+1) + 2i \cos(+1)\text{sen}(+1) + \text{sen}^2(+1)] \\ k \cdot \Delta x = +1: [-\cos^2(+1) - 2i \cos(+1)\text{sen}(+1) + \text{sen}^2(+1)] \end{cases} \quad (29)$$

It is possible to see clearly that the complex numbers will cancel itself for symmetric integration limits and that this symmetric integration limits can be also used to construct centered DRP schemes.

#### 4. SIMULATION CONDITIONS

It was simulated an 1D (one dimension) acoustic pressure pulse propagation in the center of the domain, as illustrated in Fig. 1 below. As can be seen, the initial pulse decomposes into two lower pulses that propagates in opposite directions.

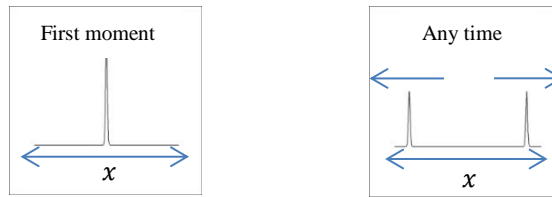


**Figure 1. Schematic shape of a 1D pressure acoustic pulse.**

In these simulations were tested several combinations of spatial and temporal schemes. Simple tests revealed the best temporal scheme. By setting the temporal scheme, it was simulated the propagation of the acoustic pulse changing spatial schemes into two different meshes: A mesh of 201 points ( $dx = 1$ ) and a refined one of 401 points ( $dx = 0.5$ ), ranging from -100 to 100 into  $x$  axis. The domain was extended from -400 to 400 and interrupted before the pulse achieve the border of the domain to avoid the pulse reflection and, consequently, contamination of the solution.

Analyzing the performance of these combinations (spatial and temporal schemes) in different mesh sizes, it was found the best spatial scheme that was set while varying the temporal schemes, with the same mesh sizes. The previous temporal scheme choice was confirmed.

Taking into account that the describe phenomenon equation are hyperbolic type, the sound propagation velocity  $c$  can not exceed the numeric solution velocity ( $dx/dt$ ):  $CFL \leq 1$ . If  $CFL$  exceeds 1 the solution will lose information and it won't represent correctly the phenomena. To avoid interference of the temporal derivative over spatial derivatives and vice versa the CFL was set 0.05. For a fixed  $CFL$  value, the temporal increase  $dt$  varies according to the mesh ( $dx$ ):

- $dx = 1 \Rightarrow dt = 0.05$ , e
- $dx = 0.5 \Rightarrow dt = 0.025$ .

According to Eq. (30):

$$CFL = c \frac{dt}{dx} \quad (30)$$

where  $c$  is the sound velocity.

The analytical solution of the pressure pulse propagation (Eq. (31)) was taken from Zhang et al. (2004).

$$p = 0.5 (1 + 0.075 \cdot e^{\left( (-\log 2.0) \cdot \frac{(x_i - (M_x + 1)t - x_0)^2}{2} \right)}) \quad (31)$$

The initial conditions for 1D case were:

$$\begin{cases} p = 1 + 0.075 \cdot e^{-(\ln 2) \frac{(x-x_0)^2}{2}} \\ u = 0 \end{cases} \quad (32)$$

## 5. RESULTS

### 5.1. Spatial Scheme Variation – Mash of 201 Points

The graphics were constructed in order to enable a better overview of the schemes performance. The pressure absolute error in all points of the domain, in all times, until the pressure pulse reaches the border of the domain, were overlaid.

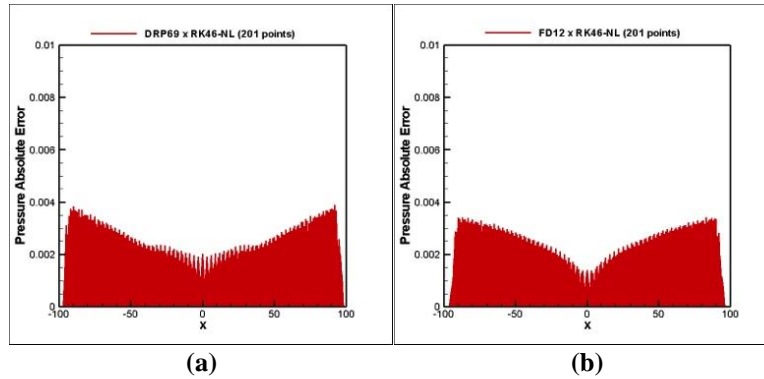


Figure 2. Pressure absolute error growth using RK46-NL (4th order optimized Runge-Kutta) and: (a) DRP69 (6th order DRP) - (b) FD12 (12th order finite differences).

It can be observed an asymptotic behavior of the error growth in this mesh of 201 points.

It is possible to see that the DRP69 (sixth order) has a performance almost equal to the FD12 (twelveth order), six order above.

### 5.2. Spatial Scheme Variation – Mesh of 401 Points

In this mesh the performance of DRP schemes decreased considerably, as shown below.

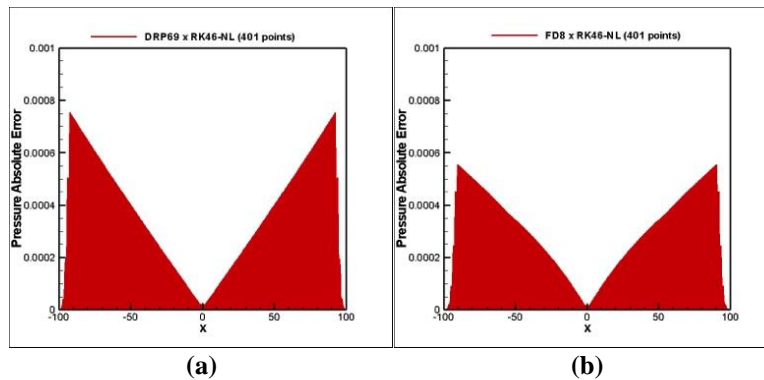
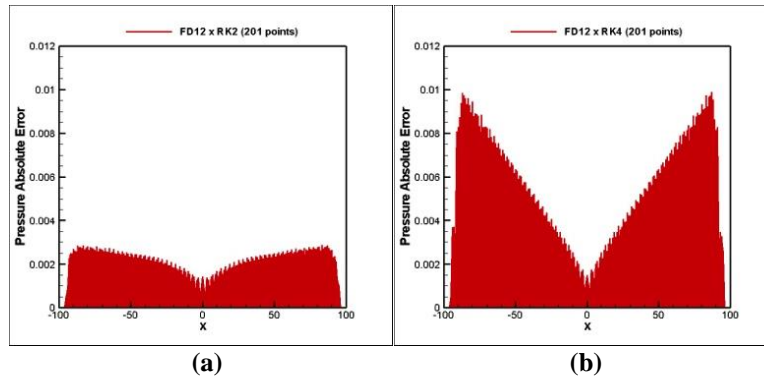


Figure 3. Pressure absolute error growth using RK46-NL (4th order optimized Runge-Kutta) and: (a) DRP69 (6th order DRP) - (b) FD8 (8th order finite differences).

### 5.3. Temporal Scheme Variation – Mesh of 201 Points

It can be seen in the next two graphics the superior performance of RK2 (2nd order Runge-Kutta) over RK4 (4th order Runge-Kutta).



**Figure 4. Pressure absolute error growth using FD12 (12th order finite differences) and: (a) RK2 (2nd order Runge-Kutta) - (b) RK4 (4th order Runge-Kutta).**

Comparing the graphics of absolute error growth of LDDRK, RK46-NL, and RK2 it shows that RK2 has the lower error and the lower growing error velocity (inclination of the tangent).

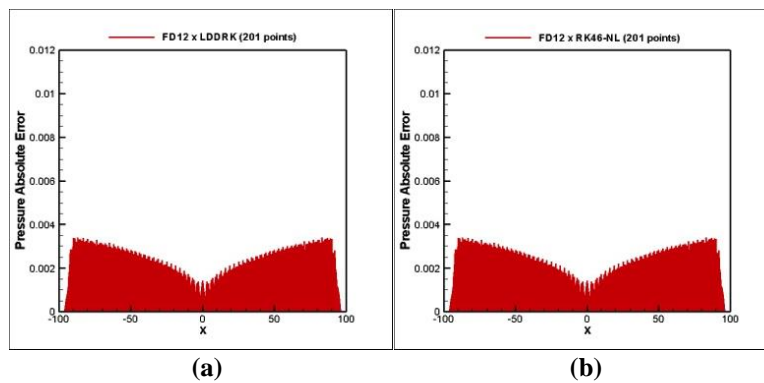


**Figure 5. Pressure absolute error growth using FD12 (12th order finite differences) and: (a) LDDRK (4th order optimized Runge-Kutta) - (b) RK46-NL (4th order optimized Runge-Kutta).**

In the mesh of 201 points RK2 revealed an outstanding superior performance over the optimized aeroacoustic temporal schemes (LDDRK and RK46-NL).

#### 5.4. Temporal Scheme Variation – Mesh of 401 Points

Under this mesh the graphics show that the optimized aeroacoustic temporal schemes (LDDRK and RK46-NL) achieved much better performance than RK2, but RK2 still got superior performance over RK4.

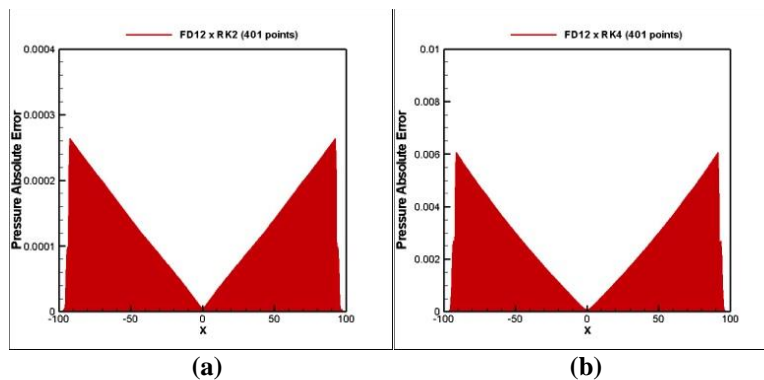


**Figure 6. Pressure absolute error growth using FD12 (12th order finite differences) and: (a) RK2 (2nd order Runge-Kutta) - (b) RK4 (4th order Runge-Kutta).**

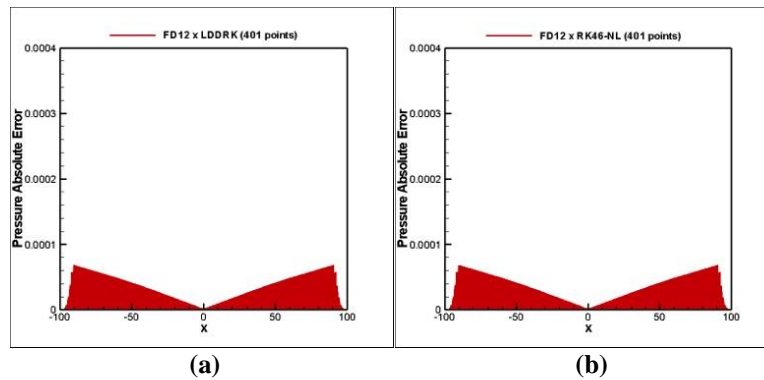


**Figure 7. Pressure absolute error growth using FD12 (12th order finite differences) and: (a) LDDRK (4th order optimized Runge-Kutta) - (b) RK46-NL (4th order optimized Runge-Kutta).**

Note that the graphics for RK2 and RK4 have different full scales. RK2 is one order of magnitude lower. The mesh refining increased the performance of the methodology.

## 6. CONCLUSION

This work has shown the need for use high order schemes in CAA, even using optimized schemes for acoustic propagation. A refined grid contributed significantly to reduce the spurious waves within the numerical procedure. The Runge-Kutta 2nd order shows an outstanding efficiency over Runge-Kutta 4th order in all simulations. This behavior must be investigated for further work in this issue. When the mesh was refined DRP schemes performance dropped in comparison to finite differences schemes, but in general terms, both DRP and finite differences schemes performed well in acoustic propagation.

## 7. ACKNOWLEDGEMENTS

Thanks to the Faculty of Mechanical Engineer and the Laboratory of Fluid Mechanics (MFlab) of the Federal University of Uberlândia (UFU).

## REFERENCES

- Berland, Julien, Bogey, Christophe, Bailly, Christophe, 2006, “Low-Dissipation and Low-Dispersion Fourth-Order Runge–Kutta Algorithm”, *Computers & Fluids*, 35, p. 1459–1463.
- Hu, F. Q., Hussaini, M. Y., Manthey, J. L., 1996, “Low-Dissipation and Low-Dispersion Runge–Kutta Schemes for Computational Acoustics”, *Journal of Computation Physics*.124, p. 177- 191.
- Mainieri, P.A. Jr, Almeida, O., Silveira, A. N., 2013, “Avaliação da Propagação Acústica Utilizando Diferenças Finitas Tradicionais e DRP”, Tese de Mestrado, Universidade Federal de Uberlândia, Uberlândia.
- Tam, C. K. W., Webb, J. C., 1993, “Dispersion-Relation-Preserving Finite Difference Schemes for Computational Acoustic”, *Journal of Computation Physics*, 107, p. 262- 281.
- Zhang, X., Blaisdell, G. A., Lyrantzis, A. S., December 2004, “High-Order Compact Schemes With Filters on Multi-block Domains”, *Journal of Scientific Computing*, Vol. 21, No. 3.

## AUTHORIAL RESPONSABILITY

The authors are solely responsible for the content of this work.